University of Rhode Island

DigitalCommons@URI

9-22-2020

Average Friction Factors of Choked Gas Flow in Microtubes

D. Kang
Kagoshima University

C. Hong
Kagoshima University

D. Rehman
Alma Mater Studiorum Università di Bologna

G. L. Morini
Alma Mater Studiorum Università di Bologna

Y. Asako
Universiti Teknologi Malaysia Kuala Lumpur

See next page for additional authors

Follow this and additional works at: https://digitalcommons.uri.edu/mcise_facpubs

Average Friction Factors of Choked Gas Flow in Microtubes

Creative Commons License

Authors

D. Kang, C. Hong, D. Rehman, G. L. Morini, Y. Asako, and M. Faghri

Average Friction Factors of Choked Gas Flow in Microtubes

Average Friction Factors of Choked Gas Flow in Microtubes

D Kang [1] , C Hong [1, 4*] , D Rehman [2] , G L Morini [2] , Y Asako [3] , M Faghri [4]

[1] Department of Mechanical Engineering, Kagoshima University, 1-21-40 Korimoto, Kagoshima 890-8580, Japan

[2] Microfluidics Laboratory, Department of Industrial Engineering (DIN), University of Bologna, Via del Lazzaretto 15/5, 40131 Bologna, Italy

[3] Department of Mechanical Precision Engineering, Malaysia-Japan International Institute of Technology, University Technology Malaysia, Jalan Sultan Yahya Petra, 54100 Kuala Lumpur, Malaysia

[4] Department of Mechanical, Industrial and Systems Engineering, University of Rhode Island, Kingston, RI, 02881, USA

[*] Corresponding author e-mail: hong@mech.kagoshima-u.ac.jp

Abstract. A micro-tube passage is a basic and important element in the design of micro heat exchangers and for this reason during the last decade a series of investigations have been made with the aim to clarify the main scaling effects playing an important role in microtubes. In this paper, a combined analysis of numerically and experimentally obtained average friction factors in microtubes under the situation of under-expanded (choked) gas flow is presented. The working fluid (nitrogen) passes through the microtube and discharges into the atmosphere under an increasing inlet pressure. Experiments and numerical computations are performed for microtubes with 249 and 528.9 μm in diameter, by varying the aspect ratio (i.e. length/diameter) from 100 to 200. The numerical methodology to solve the governing equations is based on the Arbitrary-Lagrangian-Eulerian (ALE) method. In order to capture the under-expansion characteristics of the flow during choking, the computational domain is extended in the downstream region beyond the microtube outlet. Both experimental and numerical results were obtained for a wide range of Mach number and Reynolds number. In the previous study, it was demonstrated how the outlet Mach number can be expressed as a function of the tube diameter under choked conditions. In this paper, a data reduction procedure for the estimation of the average friction factor between the inlet and the outlet of the microtube is proposed for choked flows in which the outlet gas temperature and pressure are obtained by using the outlet Mach number calculated numerically as a function of the microtube diameter. It is demonstrated how this data reduction method allows an accurate calculation of the average friction factors in microtubes by using a limited number of parameters which are easy to measure. The results obtained in this way are in good agreement with the numerical predictions as well as with the most common empirical correlations.

1. Introduction

A microtube passage is a basic and important element to design micro heat exchangers and for this reason during the last decade a series of investigations have been made with the aim to clarify the main scaling effects playing a role in micro-tubes. Since the pioneer work of Tuckerman and Pease[1], many experimental and numerical investigations on gas flow in a micro-channel or micro-tube have been undertaken [2~4]. The pressure loss determined by a friction factor between two point is one of significant factors to design micro-channel lines for heat exchangers. The friction factor for gases with large variations in the physical properties flowing through channels was obtained under the assumption of isothermal flow by most of the researchers [2~7] due to the measurement limitation of gas temperature flowing through a channel.

In a high-speed microchannel gas flow, a large expansion occurs near the outlet and the pressure gradient along the length is not constant with a significant increase near the outlet. This results in flow

acceleration and a decrease in gas temperature. Therefore the friction factor of microchannel gas flow should be obtained with measuring both the pressure and temperature. In actual situation, micro-channel gas flow does not stay isothermal and shows a strong decrease in temperature near the outlet for adiabatic walls. In terms of measuring the outlet gas temperature, placing a thermocouple in the outlet jet will measure a value between static and total temperature, and direct measurement is still challenging [8]. Fortunately for an adiabatic flow, gas static temperature estimation at the outlet of a micro-channel can be done using a quadratic equation proposed by Kawashima and Asako [9]. A new data reduction methodology for the average friction factor calculation between inlet and outlet considering the effect of a decrease in gas temperature has been developed by Hong et al. [10].

Rehman et al. [8] experimentally and numerically investigated the average friction factor along adiabatic microchannels with compressible gas flows including choking flow regime. They reported that both the assumption of perfect expansion and consequently wrong estimation of average temperature between inlet and outlet of a microchannel can be responsible for an apparent increase in experimental average friction factor in choked flow regime.

This is the motivation of the present study to experimentally and numerically investigate the average friction factors in microtubes under the situation of under-expanded (choked) gas flow.

2. Experimental setup

2.1. Micro-tube

The present experiments were carried out using four fused silica tubes. The tubes inner diameters were measured by flowing water in the tubes. The details about the diameter measurement are documented in our previous paper by Asako et al. [11]. The diameters were measured as 249 μm and 528.9 μm, by varying the aspect ratio (i.e. length/diameter) from 100 to 200.

Since the effect of inner surface roughness on micro-tube flows is relatively large compared with conventional tube flows, the inner surface roughness of microtubes used for the experiment were measured. In order to measure the roughness of the inner surface of the tube, a part of the micro-tube is cut. The arithmetic mean heights of the surface (S_a) of the micro-tubes were measured with a 3D laser scanning confocal microscope for profilometry (Keyence, VK-X260). The microscopic image of one of the roughness features is shown in figure 1. The arithmetic mean heights measured from $D = 528.9$ μm tested in this study is 0.062 μm. The values of the inner relative surface roughness of the microtubes are less than 0.01 %. Therefore inner surfaces of the microtubes seem to be smooth. Table 1 gives the detail dimensions and surface roughness of the microtubes.
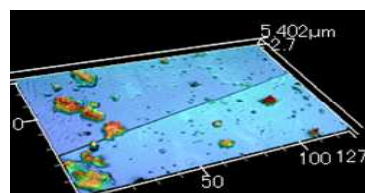
Figure 1. Laser micro-scope image of inner roughness

Table 1. Micro-tube dimensions

Micro-tube	D (μm)	Outer D (μm)	L (mm)	Ra (μm)
FST1	249	340	25	not measured
FST2	249	340	50	not measured
FST3	528.9	650	56	0.062
FST4	528.9	650	108	0.062

2.2. Configuration of Experimental setup
The schematic diagram of the experimental setup is shown in figure 2. Nitrogen gas is used as the test fluid in the present study. The nitrogen gas passes through a microtube and discharges into the atmosphere with increasing inlet pressure. Compressed nitrogen gas flows into a microtube through a single stage regulator, and a desiccant tube, into a flow meter (Kofloc 3100, 0~5 ℓ/min for D = 249 μm and 0~30 ℓ/min for D =528.9 μm), and the mass flow rate is measured at the upstream section of the micro-tube. A gauge pressure transducer (Krone KDM30, 0~1 MPa) and a thermocouple (K sheathed type) were inserted into the chamber at the upstream section of the micro-tube and the gas pressure and temperature in the chamber are measured.

The wall temperature was also measured with thermocouples (K bare wire type of 50 μm in wire diameter) attached to the microtube external wall at two locations near the outlet with a high conductivity epoxy.   The thermocouples were calibrated by resistance temperature detectors (RTD)with an accuracy of 0.1 ^{o}C. The data acquisition system (Eto Denki, CADAC21) automatically compensated for the temperature of thermocouple. The microtube exterior is covered with foamed polystyrene to avoid heat gain or loss from the surrounding environment. The signals from the pressure transducers, the mass flow meter and thermocouples are collected by a PC through a data acquisition system (Eto Denki, CADAC21). Uncertainties of measured data were listed in table 2.
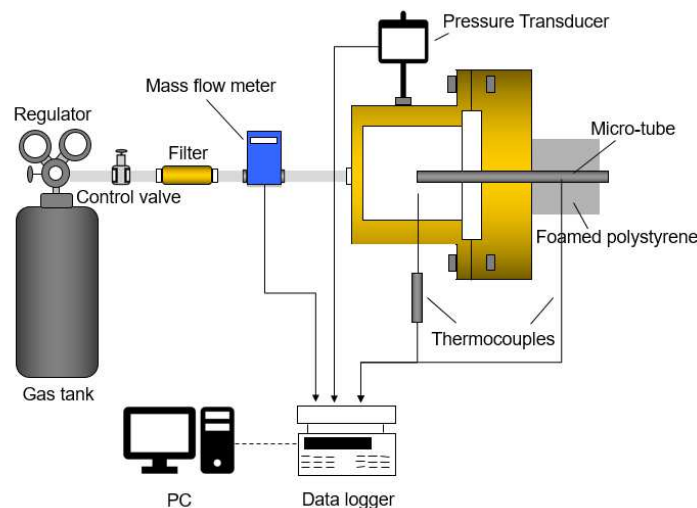
Figure 2. Schematic diagram of experimental setup

Table 2. Uncertainties of measurements

Measurements	Range	Uncertainties
Pressure (Krone KDM30)	(0~1 MPa)	(±0.25% of FS (2500 Pa))
Flow rate (KOFLOC 3100)	(0~5 L/min) (0~30 L/min)	(±1.0% of FS (0.05 L/min)) (±1.0% of FS (0.3 L/min))
Temperature (Bare wire type-T thermocouple)	(299.15~346.15K)	(±0.1 K)
(Bare wire type-K thermocouple)	(300.15~348.15K)	(±0.1 K)

3. Data reduction

3.1. Gas temperature, Reynolds number and Mach number

The static gas temperature of high speed gas flow in a microchannel could not be measured by insertion of a temperature probe into the microchannel, since the insertion of a temperature probe into a microchannel affects on fluid flow in the microchannel. The static gas temperature of high speed gas flow in a microchannel should be obtained another way to calculate friction factors and Mach number. For an adiabatic channel flow, the static gas temperatures at the outlet pressure, $T = T_{out}$ can be obtained by the following equation obtained by [9].

$$T = \frac{-1 + \sqrt{1 + 4 \times \alpha \frac{\rho_{in}^2 u_{in}^2 R^2}{2c_p p^2} \times \left(T_{in} + \frac{u_{in}^2}{2c_p} \right)}}{2 \times \alpha \frac{\rho_{in}^2 u_{in}^2 R^2}{2c_p p^2}} \tag{1}$$

where ρ_{in}, u_{in}, and T_{in} are density, velocity and temperature at the inlet and p is the pressure at the outlet. And c_p is specific heat at constant pressure and α is kinetic energy loss coefficient which is proposed to be 2 for laminar and 1 for turbulent flows respectively.

Inlet values of velocity, density and temperature are obtained with isentropic process between the inlet and the stagnation area [12]. Furthermore, the inlet pressure is also obtained by considering the minor loss of square edged type for tube entrance. Also Reynolds number and Mach number are

$$Re = \frac{\rho u D}{\mu} = \frac{4\dot{m}}{\pi \mu D} \tag{2}$$

$$Ma = \frac{u}{a} = \frac{u}{\sqrt{\gamma R T}} \tag{3}$$

where $\dot{m}$ is mass flow rate and μ is viscosity of gas.

At the outlet, equation (3) with the equation of state and mass flow rate per unit area, $\dot{G}$ (kg/(s m^2)) can be rewritten as

$$Ma_{out} = \frac{\dot{G}}{p_{out}} \sqrt{\frac{R T_{out}}{\gamma}} \tag{4}$$

And the following equation can be obtained for an adiabatic channel flow

$$T_{out} = \frac{2 T_{stg}}{(\gamma - 1) Ma_{out}^2 + 2} \tag{5}$$

Then, the outlet pressure is

$$p_{out} = \frac{\dot{G}}{Ma_{out}} \sqrt{\frac{R T_{out}}{\gamma}} = \frac{\dot{G}}{Ma_{out}} \sqrt{\frac{2 R T_{stg}}{\gamma[(\gamma - 1) Ma_{out}^2 + 2]}} \tag{6}$$

where γ is specific heat ratio.

If the outlet Mach number is given, the outlet pressure and temperature can be determined from equation (5) and (6).

3.2. Average friction factor

In the case of microchannel gas flow at high speed, the large expansion occurs near the outlet and the pressure gradient along the length is not constant and increases near the outlet. This results in flow acceleration and decrease in bulk temperature. Therefore the both pressure and temperature are required to obtain the friction factor of the microchannel gas flow. As mentioned above, Kawashima and Asako [9] found that the gas temperature can be determined by the pressure under the assumption of one dimensional flow in an adiabatic channel (Fanno flow) to obtain the friction factor considering the effect of decrease in gas temperature. Then, the four times of Fanning friction factor (hereinafter referred to as the Fanning friction factor) for the Fanno flow defined by Kawashima and Asako [9] defined the four multiples of the Fanning friction factor for an adiabatic wall (Fanno flow) as

$$f_{\mathrm{f}} = \frac{4\tau_{\mathrm{w}}}{\frac{1}{2}\rho u^2} = \frac{2D}{p}\left(\frac{\mathrm{d}p}{\mathrm{d}x}\right) - \frac{2Dp}{\rho^2 u^2 RT}\left(\frac{\mathrm{d}p}{\mathrm{d}x}\right) - \frac{2D}{T}\left(\frac{\mathrm{d}T}{\mathrm{d}x}\right) \tag{7}$$

where τ_{w} is shear stress on a wall.

The temperature at x is a function of the pressure at x for an adiabatic wall. Substituting the temperature, T obtained by Eq. (1) into Eq. (4) and integrating Eq. (4) between the inlet (x_1) and outlet (x_2), the following average Fanning friction factor can be obtained as [14]:

$$f_{\mathrm{f,ave}} = \frac{1}{x_2 - x_1}\int_{x_1}^{x_2} f_{\mathrm{f}}\,\mathrm{d}x = \frac{D}{x_2 - x_1}\left\{\int_{x_1}^{x_2}\left(\frac{2}{p}\,\mathrm{d}p\right) - \int_{x_1}^{x_2}\left(\frac{2p}{\rho^2 u^2 RT}\,\mathrm{d}p\right) - \int_{x_1}^{x_2}\left(\frac{2}{T}\,\mathrm{d}T\right)\right\} \tag{8}$$

$$= \frac{D}{x_2 - x_1}\left[\begin{array}{c}-2\ln\dfrac{p_1}{p_2} + 2\ln\dfrac{T_1}{T_2} - \dfrac{1}{\left(\rho_{\mathrm{in}}^2 u_{\mathrm{in}}^2 R\times\left(T_{\mathrm{in}} + \dfrac{u_{\mathrm{in}}^2}{2c_{\mathrm{p}}}\right)\right)} \\[2em] \times\left\{\dfrac{p_2^2 - p_1^2}{2} + \dfrac{B^2}{2}\ln\dfrac{p_2 + \sqrt{p_2^2 + B^2}}{p_1 + \sqrt{p_1^2 + B^2}} + \dfrac{1}{2}\left(p_2\sqrt{p_2^2 + B^2} - p_1\sqrt{p_1^2 + B^2}\right)\right\}\end{array}\right]$$

where

$$B^2 = 4\times\alpha\,\frac{\rho_{\mathrm{in}}^2 u_{\mathrm{in}}^2 R^2}{2c_{\mathrm{p}}}\times\left(T_{\mathrm{in}} + \frac{u_{\mathrm{in}}^2}{2c_{\mathrm{p}}}\right) \tag{9}$$

4. Results and discussion

The experiments to obtain average Fanning friction factors of nitrogen gas flows were carried out using four silica micro-tubes. The tested stagnation pressure range and the obtained Reynolds number are shown in table 3.

In order to make a comparison with the experimental results, numerical computations based on the Arbitrary-Lagrangian-Eulerian (ALE) method were also conducted for a fused silica tube of $D = 249$ μm (FST1 and FST2) whose boundary conditions are identical to the experimental conditions. A detailed description of the numerical computation is documented in the previous work [13] and will not be repeated here. Only the brief description is reported here. The Lam-Bremhorst Low-Reynolds number (LB1) model was employed to evaluate eddy viscosity coefficient and turbulent energy since LB1 model is widely used and very stable. The numerical computations were performed under the assumption of steady, axisymmetric flow and an ideal gas. It is also assumed that the velocity, pressure, temperature and density profiles at the inlet are uniform. The thermal boundary condition on the wall is adiabatic. The numerically obtained Reynolds numbers are also tabulated in table 3.

Table 3. Tube diameter, length, p_{stg} and Re

Microtube		D (μm)	L (mm)	p_{stg} (kPa)	Re
Experiments	FST 1	249	25	100 ~ 700	574 ~ 13389
	FST 2	249	50	100 ~ 1100	334 ~ 17297
	FST 3	528.9	56	102 ~ 1100	640 ~ 45737
	FST 4	528.9	108	104 ~ 1198	608 ~ 38428
Numerical Calculations	FST 1	249	25	200 ~ 1100	3155 ~ 21202
	FST 2	249	50	200 ~ 1100	2501 ~ 16718

4.1. Mass flow rate

The measured mass flow rates for the two microtubes of L=25 mm and 50 mm of D = 249 μm are plotted in figure 3 as a function of the stagnation pressure using square data markers. The mass flow rates obtained numerically for the micro-tube of D = 249 μm are also plotted in the figure using solid circle data markers. The mass flow rate increase with an increase in the stagnation pressure since the gas at the outlet is discharged into the atmosphere under an increasing inlet pressure. And it increases with a different slope in the range of p_{stg} > 200 kPa since the flow transits to turbulent flow from laminar flow regime. Then Reynolds number is in range of 2000 < Re < 2500. And this will be discussed in the friction factor section. Both experimental and numerical mass flow rates for the micro-tube of D = 249 μm are in excellent agreement. Qualitatively similar results for the micro-tubes of L=56 mm and 108 mm of D = 528.9 μm are obtained.

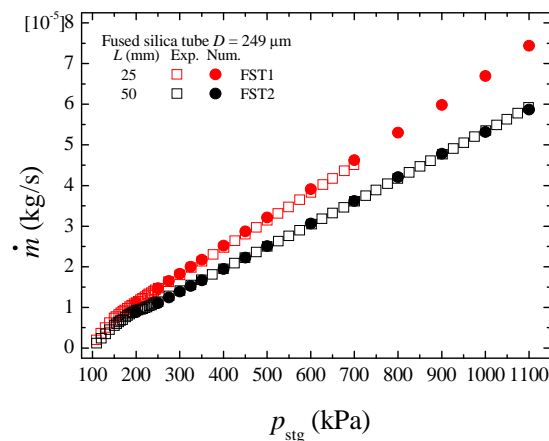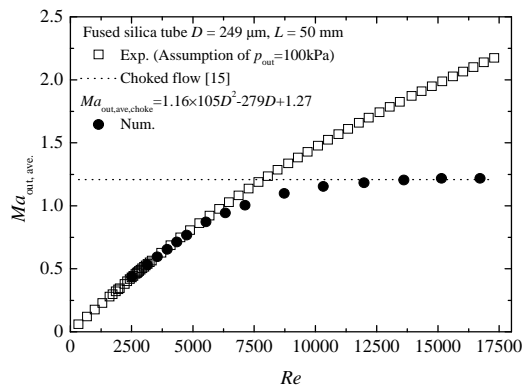**Figure 3.** Mass flow rates for L =25 mm and 50 mm of D = 249 μm


Figure 4. Outlet Mach number for D = 249 μm and L = 50 mm

4.2. Outlet Mach number

The outlet Mach numbers obtained from equation (3) under the assumption of $p_{out} = p_{atm}$ (atmospheric pressure) for the micro-tube of D = 249 μm and L = 50 mm are plotted in figure 4 as a function of Re. The outlet Mach numbers obtained numerically are also plotted in the figure using solid circle data markers. They keep on increasing with the Reynolds number in the range of $Re \leq 10000$. And they get to an almost constant value in the range of Re > 10000. At this point, flow starts to choke and the outlet Mach number reaches a constant value close to 1 (i.e., in this case $Ma_{out} \approx 1.21$ in the range of Re > 10000). An explanation of supersonic jet at the exit of constant area ducts has been presented by Lijo et al. [14]. Numerical works of Kawashima et al. [15] and Hong et al. [16] showed that the outlet Mach number can go higher than its maximum limit of 1. This happens due to shear thinning of the boundary layer close to the outlet of a microtube that serves as de-Laval nozzle for incoming high subsonic jet of gas flow. Kawashima et al. [15] reported the average Mach number at the outlet plane

of the choked flow depends on the tube diameter and proposed a correlation for the average Mach number at the outlet plane of the choked flow as

$$Ma_{out,ave,choke} = 1.16 \times 10^5 D^2 - 279D + 1.27 \tag{10}$$

The outlet Mach number obtained from equation (10) for $D = 249$ μm is plotted in the figure by the dotted line ($Ma_{out,ave,choke} = 1.208$). This value almost coincides with numerically obtained outlet Mach numbers in the range of $Re > 10000$. At maximum Re, even though the flow is choked, the experimentally obtained outlet Mach number reaches as high as 2.2 because of the assumption of $p_{stg} = p_{atm}$. In actual situation, when the flow is choked, the outlet flow becomes under-expanded and the outlet pressure is higher than the atmosphere pressure ($p_{out} > p_{atm}$). Then, the outlet Mach number and the gas temperature remain nearly unchanged [8]. Therefore the above correlation of $Ma_{out,ave,choke}$ (equation (10)) [15] is employed to determine the values of pressure and gas temperature at the outlet (equations (5) and (6)) when the flow is choked.
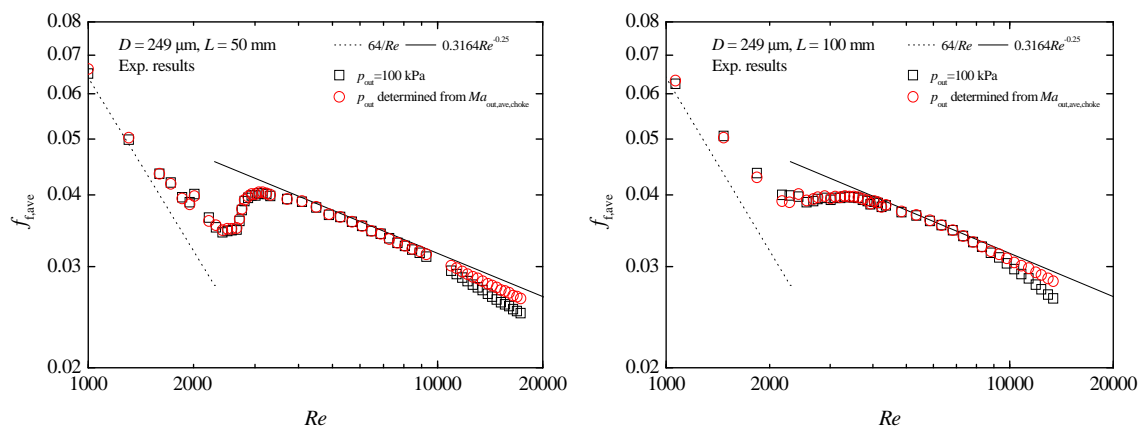
(a) $L = 25$ mm   (b) $L = 50$ mm

Figure 5. Average friction factor vs Re for $D = 249$ μm
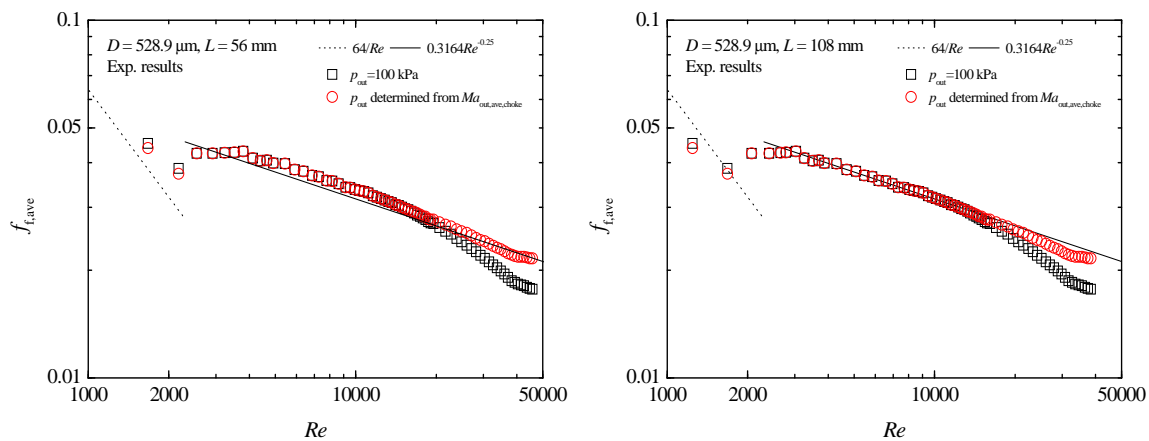
(a) $L = 56$ mm   (b) $L = 108$ mm

Figure 6. Average friction factor vs Re for $D = 528.9$ μm

4.3. Average friction factor

The average Fanning friction factors between the inlet and outlet, $f_{f,ave}$ for all tubes (FST1~4) were obtained by equation (8) with the assumption of $p_{out} = p_{atm}$. The values of $f_{f,ave}$ are plotted by squares on a Moody chart in figures 5 and 6. The values of $f_{f,ave}$ obtained with p_{out} determined by equation (10) are also plotted by circles in the figures when the flow is choked. The dotted line and the solid line in the figures represent the values obtained by the theoretical formula ($f=64/Re$) and

$f=0.3164/Re^{0.25}$ (*Blasius* equation) for incompressible flow theory, respectively. As can be seen in the figures the flow transits from laminar flow to turbulent flow in the range of $2000 < Re < 4000$ the same as conventional sized tubes. In the laminar flow regime on figure 5 (a) and (b), the values of $f_{f, ave}$ deviate more and more from that of an incompressible flow with an increasing in Reynolds number because of the compressibility effect. In the case of the turbulent flow regime before flow choking (unchoked turbulent flow regime) on the figures 5 and 6, the values of $f_{f, ave}$ nearly coincide with *Blasius* equation. However, in the case of the turbulent flow regime after flow choking (choked turbulent flow regime), the values of $f_{f, ave}$ obtained under the assumption of $p_{out}= p_{atm}$ deviate in the lower direction from *Blasius* equation with an increase in Reynolds number since the assumption of $p_{out} = p_{atm}$ is not valid with flow choking. The values of $f_{f, ave}$ obtained with p_{out} determined by equation (10) on figure 5 (a) and (b) are slightly lower than *Blasius* equation and the values on figure 6 (a) and(b) almost coincide with *Blasius* equation. As a result of that, when the flow is choked, the gas velocity (Mach number) and gas temperature at the outlet remain unchanged, and the outlet pressure is higher than the back pressure (atmospheric pressure) with an increase in Reynolds number. However, the outlet temperature obtained under the assumption of $p_{out} = p_{atm}$ does not remain unchanged rather steeply decreases. Therefore in the choked turbulent flow regime, the arithmetic average gas temperature between the inlet and outlet decreases and $f_{f,ave}$ decreases. As mentioned above, $Ma_{out,ave,choke}$ considering flow choking is a specific value represented as a function of tube diameter. The outlet pressure determined by $Ma_{out,ave,choke}$ is higher than atmospheric pressure and the outlet gas temperature determined by it remains unchanged. Then, $f_{f,ave}$ is slightly lower than *Blasius* equation or nearly coincide with *Blasius* equation.

5. Conclusions
The average Fanning friction factors between the inlet and outlet of microtubes, $f_{f,ave}$ are obtained under the assumption of $p_{out} = p_{atm}$ and with p_{out} determined by $Ma_{out,ave,choke}$ considering flow choking. The following conclusions were reached.

(1) When the flow is choked, the outlet Mach numbers (gas velocity) obtained numerically remain unchanged with an increase in Reynolds number. However, they obtained under the assumption of $p_{out} = p_{atm}$ reaches as high as 2.2 for $D = 249$ μm.
(2) In the unchoked turbulent flow regime, the values of $f_{f,ave}$ obtained experimentally for all microtubes and *Blasius* equation are in excellent agreement.
(3) In the choked turbulent flow regime, the values of $f_{f, ave}$ obtained under the assumption of $p_{out}= p_{atm}$ deviate in the lower direction from *Blasius* equation with an increase in Re since the assumption of $p_{out} = p_{atm}$ is not valid with choked flows. However, the values of $f_{f,ave}$ obtained by the outlet pressure determined by $Ma_{out,ave,choke}$ are slightly lower than *Blasius* equation or nearly in agreement with *Blasius* equation.

6. References
[1]   Tuckerman D B and Pease R F W 1981 *IEEE Electron Device Letter* **EDL-2** 126-129
[2]   Wu P and Little W A 1984 *Cryogenics* **24** 415~420
[3]   Yang C, Chen C, Lin T and Kandlikar S G 2012 *Exp. Therm. Fluid Sci.* **37** 12–18.
[4]   Morini G L, Lorenzini M, Salvigni S and Spiga M 2009 *Microfluidics and nanofluidics* **7**, no. 2 181-190.
[5]   Turner S E, Lam L C, Faghri M and Gregory O T 2004 *J. Heat Transfer* **127** 753–763.
[6]   Tang G H, Li Z, He Y L and Tao W Q 2007 *Int. J. Heat Mass Transfer* **50** 2282–2295.
[7]   Hong C, Yamada T, Asako Y and Faghri M 2012 *Int. J. Heat Mass Transfer* **55** 4397–4403.
[8]   Rehman D, Morini, G L and Hong C 2019 *Micromachines* **10** 171
[9]   Kawashima D and Asako Y 2014 *Int. J. Heat Mass Transfer* **77** 257–261.
[10]   Hong C, Asako Y, Morini G L and Rehman D 2019 *Int. J. Heat Mass Transfer* **129** 427-431
[11]   Asako Y, Nakayama K and Shinozuka T 2005 *Int. J. Heat Mass Transfer* **48** 4985-4994.
[12]   Karki K C 1986 A Calculation Procedure for Viscous Flows at All speeds in Complex Geometries, Ph.D. Thesis, University of Minesota

[13]   Hong C, Tanaka G, Asako Y and Katanoda H 2018 *Int. J. Heat Mass Transfer* **121** 187-195.

[14]   Lijo V, Kin H D and Setoguchi T 2010 *IMechE Part G J. Aerosp Eng.* **224**, 1151–1162

[15]   Kawashima D, Yamada T, Hong C and Asako Y 2016 *IMechE Part C J. Mech. Eng. Sci.* **19** 3420–3430

[16]   Hong C, Yoshida Y, Matsushita S, Ueno I and Asako Y 2015 *Bulletin of the JSME Journal of Thermal Science and Technology* **Vol.10**, No. 2, p 1-9